

The Initiation and Propagation of Dynamic Abnormal Grain Growth in Molybdenum



PHILIP J. NOELL, DANIEL L. WORTHINGTON, and ERIC M. TALEFF

Plastic straining can initiate and propagate abnormal grains at temperatures significantly lower than is possible by static annealing. This phenomenon is termed dynamic abnormal grain growth (DAGG). Experiments that produce DAGG in commercial-purity molybdenum sheet materials are used to study the initiation and propagation of abnormal grains by plastic straining at temperatures from 1673 K to 2073 K (1400 °C to 1800 °C). The minimum strain necessary to initiate DAGG, termed the critical strain, decreases approximately linearly with increasing temperature. The variation in critical strain values observed at a single temperature and strain rate is well described by a normal distribution. An increased fraction of grains aligned with the $\langle 110 \rangle$ along the tensile axis, a preferred orientation for DAGG grains, appears to decrease the critical strain for DAGG initiation. DAGG grains preferentially grow into the finest-grained polycrystalline regions, which suggests that the driving force for DAGG propagation is primarily from grain-boundary curvature. No effects of local crystallographic texture variation on growth are evident in microstructures containing DAGG grains. Together, these observations support the hypothesis that plastic straining during DAGG acts primarily to increase boundary mobility, rather than to increase the driving force for boundary migration.

DOI: 10.1007/s11661-015-3188-6

© The Minerals, Metals & Materials Society and ASM International 2015

I. INTRODUCTION

ABNORMAL grain growth (AGG) is the process of one or a few grains rapidly growing in size by consuming many surrounding smaller grains.^[1–3] This typically produces a microstructure that contains one or a few grains many times larger than the original grain size.^[4–6] In the most extreme case, AGG can produce a single crystal.^[7,8] For some applications, such as directionally oriented silicon steels, the large grains produced by AGG are very desirable.^[9] However, AGG is typically undesirable in structural materials because the resulting large grains reduce part strength.^[10] These effects motivate our desire to understand AGG phenomena sufficiently to both predict and control them. The current understanding of these phenomena is, unfortunately, incomplete.^[11] The present study endeavors to extend our understanding of the subset of AGG phenomena that occur during plastic straining at elevated temperatures.

Two distinct categories of AGG phenomena are known: static abnormal grain growth (SAGG) and dynamic abnormal grain growth (DAGG).^[12–14] SAGG is defined as AGG that occurs without any concurrent plastic straining, *i.e.*, under static conditions.^[12] SAGG in bulk metallic materials is controlled primarily by a

combination of grain-boundary energy,^[15,16] stored dislocation energy,^[17,18] and texture.^[1,19,20] Most investigations of AGG described in the literature deal exclusively with SAGG. DAGG is a recently discovered phenomenon^[12] defined as AGG that occurs during concurrent plastic straining, *i.e.*, under dynamic conditions. Several important features distinguish DAGG from SAGG. The most striking are that DAGG occurs at much lower temperatures and proceeds more rapidly than SAGG.^[12–14] DAGG has been definitively observed in the two BCC refractory metals Mo and Ta.^[12–14] In Mo, abnormal grains were grown by DAGG at rates of up to 0.5 mm s⁻¹ and to lengths as long as 10 cm.^[13] This maximum size was restricted only by the physical limitations of the testing apparatus.

DAGG is illustrated through the example shown in Figure 1. These data are from tensile tests of a commercial-purity Mo sheet conducted at a constant true-strain rate of 10⁻⁴ s⁻¹ and a constant temperature of 1923 K (1650 °C). As the true-stress vs true-strain plot in Figure 1(a) demonstrates, this material initially displays the high-temperature polycrystalline creep deformation expected for these conditions.^[21] However, after accumulating a critical strain, ϵ_c , a dramatic drop in flow stress occurs. The drop in flow stress from the value labeled as σ_c corresponds with the initiation of DAGG. If tensile straining is terminated shortly after ϵ_c , DAGG will typically cease, and a DAGG grain, or grains, that has partially consumed the gage region will remain. Such a case is shown in the polished and etched tensile coupon of Figure 1(b). This demonstrates the importance of concurrent plastic deformation to DAGG. If tensile straining were continued, the DAGG grain would continue to propagate along the gage length

PHILIP J. NOELL, Current Student, and ERIC M. TALEFF, Professor of Mechanical Engineering, are with the University of Texas at Austin, 204 East Dean Keeton St., Stop C2200, Austin, TX 78712-1591. Contact e-mail: philip.noell@utexas.edu DANIEL L. WORTHINGTON, Former Student, is with Fujifilm Dimatix, Inc., 2250 Martin Avenue, Santa Clara, CA 95050.

Manuscript submitted June 19, 2015.

Article published online October 14, 2015

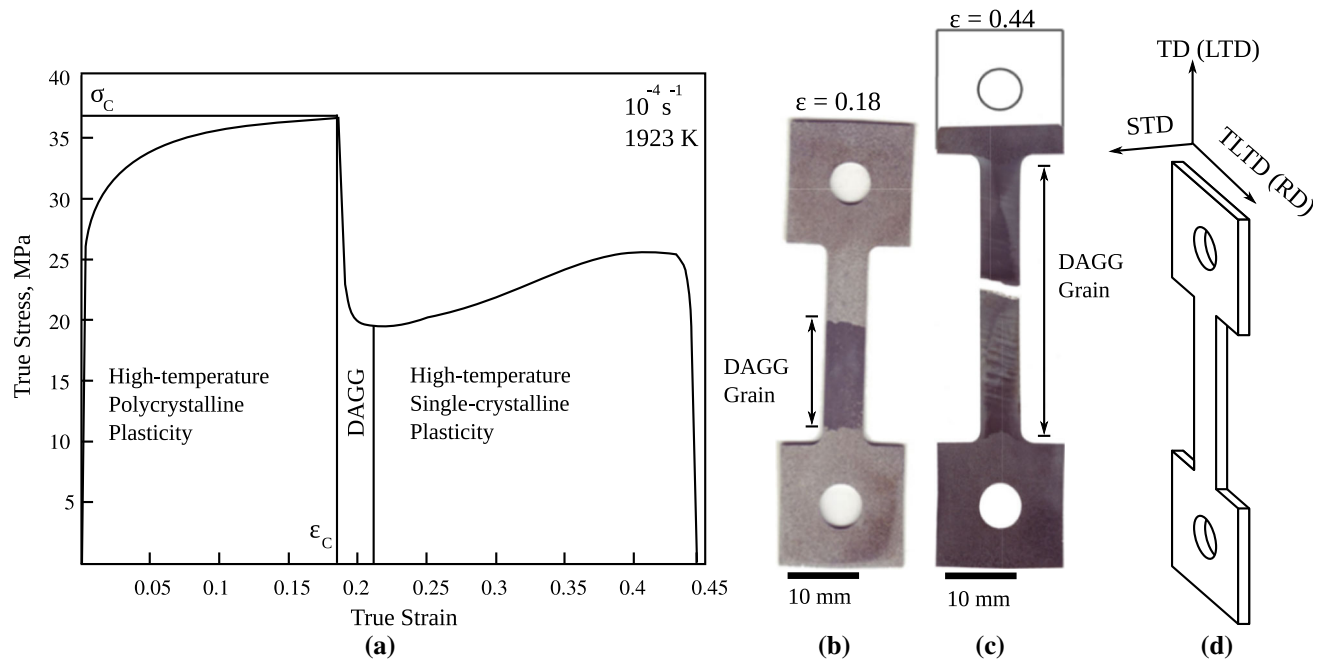


Fig. 1—Data from a constant true-strain rate tensile test at 10^{-4} s^{-1} and 1923 K (1650 °C) of the commercial-purity Mo PMB material that produced DAGG are provided. Shown are (a) a graph of true stress vs true strain, (b) a macroetched tensile specimen tested until shortly after DAGG initiation, and (c) a macroetched tensile specimen with a DAGG grain that was strained until specimen rupture. The schematic shown in (d) indicates the orientation of the specimen's tensile direction (TD) and tensile long transverse direction (TLTD) with respect to the sheet's final rolling direction (RD) and long transverse direction (LTD).

until its polycrystalline microstructure was completely consumed. Once an abnormal grain, or grains, completely consumes the polycrystalline microstructure of the gage region, DAGG is complete. As shown by the polished and etched tensile coupon in Figure 1(c), tensile deformation after DAGG completion plastically deforms the abnormal grain(s) until specimen rupture. The DAGG grain does not penetrate significantly into the tensile coupon grip, where little plastic straining occurs.

DAGG was previously observed in two Mo sheet materials.^[13] These sheet materials were designated Mo AM and Mo PM because they were produced by arc-melting and powder-metallurgy techniques, respectively. DAGG was also observed in a Ta sheet material.^[14] DAGG in all these materials has the following characteristics in common:

1. The distance a DAGG grain boundary propagates is a direct function of plastic strain accumulation during the stress drop, not time.
2. DAGG grains are preferentially oriented with the $\langle 110 \rangle$ approximately along the tensile direction.
3. DAGG is impeded by large grains.
4. ϵ_c does not vary significantly with strain rate within the range of strain rates studied.

ϵ_c was observed to decrease with increasing temperature in Mo. Although this relationship was not observed in Ta, it is thought that excessive normal grain growth prior to DAGG initiation in Ta is the reason for this negative result.

Many unanswered questions remain for the mechanisms that control DAGG initiation and propagation. This study is intended to answer the following specific questions regarding DAGG:

1. How does temperature affect ϵ_c ?
2. What is the statistical variation in ϵ_c for constant test conditions?
3. How do the initiation and growth of DAGG vary with local microstructure?

A commercial-purity Mo sheet material previously shown to exhibit negligible normal grain growth at temperatures up to 2073 K (1800 °C)^[13] was selected to study these questions. The use of this material avoids the complications caused by normal grain growth prior to DAGG and facilitates comparisons between DAGG behaviors at different temperatures.

II. EXPERIMENTAL PROCEDURES

High-temperature tensile tests were performed on a commercial-purity Mo sheet fabricated using powder-metallurgy techniques and meeting the ASTM B 386, Grade 361 specification for commercially pure Mo.^[22] This sheet was rolled to a final thickness of 0.76 mm. Worthington *et al.*^[13] previously studied DAGG in a similar commercial-purity Mo sheet fabricated using powder-metallurgy techniques. This sheet met the same ASTM B 386, Grade 361 specification for commercially pure Mo^[22] and was rolled to the same final thickness.

To distinguish between these two materials, both obtained from the same producer, the Mo sheet material studied by Worthington *et al.*^[13] is designated Mo PMA, and the Mo sheet material of the present investigation is designated Mo PMB. Although material production of both Mo sheets may have involved cross-rolling, which is known to be the case for the Mo PMA material, the final rolling direction of each sheet was noted and used as a reference for specimen directions.

The manufacturer's maximum limits for chemical impurities in the Mo PMB powder prior to consolidation are shown in Table I by weight percent. The concentrations of the light elements C, N, O, and S in the final sheet material were determined independently using an inert-gas-fusion technique.^[23] For comparison, the chemical content of the Mo PMA material is also provided in Table I. Further information about the Mo PMA material is available in reference.^[13]

The Mo PMB sheet material was tested as pin-loaded tensile coupons machined from the as-received material with a gage length of 25.4 mm, a gage width of 6.4 mm, a radius of 1.6 mm between the grip and gage regions, and an as-received thickness of 0.76 mm. The pin diameter was 6.15 mm. The specimen tensile axis direction (TD) was perpendicular to the final sheet rolling direction (RD) for all tests; see Figure 1(d). Uniaxial tension tests were performed at a constant true-strain rate of 10^{-4} s^{-1} and constant temperatures ranging from 1673 K to 2073 K (1400 °C to 1800 °C). These tests used a computer-controlled, electromechanical testing frame fitted to a vacuum furnace. This furnace consistently achieved a vacuum of 10^{-6} Torr during testing. Tungsten heating elements inside the vacuum furnace heated specimens to each testing temperature within a few minutes. The temperature of the furnace hot zone was maintained to within ± 10 K of the set temperature. This was determined through separate temperature profiling experiments. Tensile specimens remained entirely within the furnace hot zone during testing and were attached by pins to tungsten pull rods that exited the furnace through bellows assemblies. Specimens were preheated to the testing temperatures and held for 2 hours under a light load. After 2 hours, thermal expansion of the tungsten pull rods effectively ceased. This enabled accurate calculation of specimen elongation from cross-head displacement during testing. It is important to note that, because the recrystallization

temperature of commercial-purity Mo is between 1173 K and 1473 K (900 °C and 1200 °C),^[24] all specimens were fully recrystallized prior to tensile testing.

To provide a constant true-strain rate, the cross-head displacement rate of the load frame was continuously varied through computer control during testing. It was assumed that the specimen deformed uniformly and that the volume of the specimen gage length remained constant. Measurements after testing indicate that these assumptions are valid for strains up to nearly specimen rupture. A load cell outside the furnace monitored force on the pull rods throughout each test. The displacement of the test frame cross-head was also recorded during each test. Using data from calibration experiments, these test data were corrected to remove the effects of thermal expansion in the load train and the forces from bellows that seal the entrance of the load train into the furnace. These corrected data were then used to calculate true stress and true strain throughout each test.

Forty-seven (47) tensile tests in total were conducted at temperatures from 1673 K to 2073 K (1400 °C to 1800 °C) on the Mo PMB sheet material, all at a constant true-strain rate of 10^{-4} s^{-1} . These tests are summarized in Table II. To characterize the early stages of DAGG, twenty (20) tensile tests at 1923 K (1650 °C) and six (6) tensile tests at 2073 K (1800 °C) were halted shortly after DAGG initiation. The remaining twenty-one (21) tensile tests were conducted to rupture. The tensile tests conducted to rupture are designated elongation-to-failure, EF, tests. The tensile tests halted shortly after DAGG initiation, shortly beyond ϵ_c , are designated halt tests. For the twenty-six (26) halt tests, the tensile load was continuously monitored for the sharp drop in load associated with the initiation of DAGG. When the tensile load dropped to 95 pct of its maximum value during the test, the control software program automatically unloaded the test specimen. Once unloaded, the furnace was turned off to cool the specimen while the software program continuously adjusted the cross-head position to prevent loading of the specimen during thermal contraction of the load train. These procedures were intended to preserve the microstructure produced shortly after DAGG initiation for later characterization.

Microstructures of the Mo tensile coupons were characterized after high-temperature testing using optical microscopy, scanning electron microscopy (SEM),

Table I. The Manufacturer's Reported Chemical Composition of the Mo PMB Powder Prior to Consolidation Is Listed by Weight Percent for all Elements Except C, N, O, and S

Mo PMB	Mg	Mn	Ni	Al	Cu	Pb	Ti	Ca	
	≤0.001	≤0.001	≤0.002	≤0.002	≤0.002	≤0.002	≤0.002	≤0.003	
	Si	Sn	Cr	Fe	C	N	O	S	Mo
	≤0.003	≤0.003	≤0.005	≤0.005	10 ppm	10 ppm	40 ppm	10 ppm	bal.
Mo PMA	Mg	Mn	Ni	Al	Na	W	Co	Ca	
	0.0004	0.0001	0.0002	0.0016	0.0001	0.0034	0.0001	0.0005	
	Si	K	Cr	Fe	C	N	O	S	Mo
	0.0023	0.0002	0.0007	0.0022	< 10 ppm	< 10 ppm	34 ppm	—	bal.

The composition of the Mo PMA sheet is listed by weight percent for all elements except C, N, O, and S. The measured concentrations of C, N, O, and S in both sheets are shown in parts per million (ppm) by weight.

Table II. The Elongation-to-Failure (EF) and Halt Tests for the Mo PMB Material Are Enumerated by Test Temperature

T (K)	T (°C)	Total Tests	Halt Tests	EF Tests	DAGG Events
1673	1400	1	0	1	0
1723	1450	2	0	2	0
1823	1550	1	0	1	1
1873	1600	1	0	1	1
1923	1650	29	20	9	29
1973	1700	2	0	2	2
2073	1800	11	6	5	11

The number of tests that produced DAGG grains are indicated. All tests were at 10^{-4}s^{-1} .

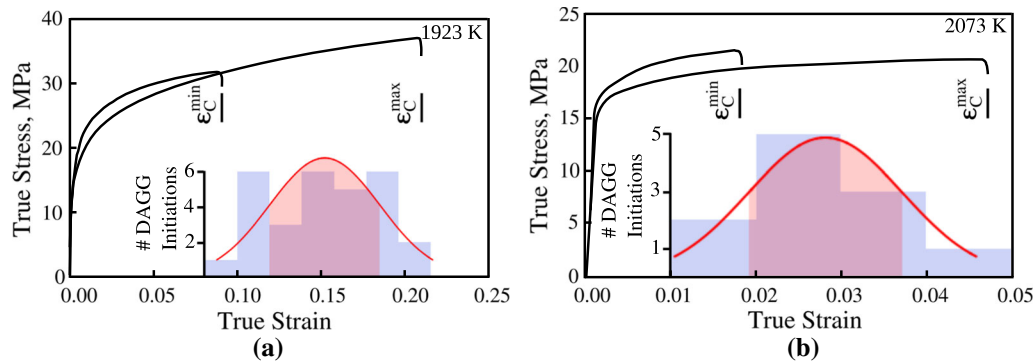


Fig. 2—True-stress vs true-strain data from tensile tests of Mo PMB at (a) 1923 K (1650 °C) and (b) 2073 K (1800 °C) are shown. Data from the tests that produced DAGG at the lowest and highest critical strains, labeled ϵ_c^{\min} and ϵ_c^{\max} , are shown for each temperature. Histograms, overlaid with probability density function curves spanning the 95 pct confidence interval, are shown under the tensile data. These histograms indicate the number of DAGG events observed that initiated within each range of true-strain values. The shaded area under each probability distribution function curve indicates the standard deviation.

and electron backscatter diffraction (EBSD). The crystallographic orientations of large individual DAGG grains were indexed using the Laue X-ray back-diffraction technique. For optical microscopy and Laue X-ray back-diffraction, tensile coupons were ground, polished, and subsequently etched in a solution of one part nitric acid, one part sulfuric acid, and three parts water, by volume. For EBSD and SEM observations, specimens were ground and polished using standard techniques, with final polishing carried out for extended times in a colloidal silica suspension. EBSD data were collected on an FEI XL30 ESEM (environmental SEM) operating at 20 kV using either Oxford HKL Channel5™ software or HKL AZtec™ software.^[25] EBSD characterization was performed using a step size of $2\ \mu\text{m}$, 8×8 binning, and a Hough space resolution of 60. Material from the grip region, which reflects the undeformed, recrystallized microstructure after time at temperature, was characterized to document the microstructure produced by static annealing. Material from the gage region was characterized to document the deformed microstructure. Average grain sizes, \bar{d} , were measured from SEM backscatter images using the lineal intercept method.^[26] Directional grain sizes were also measured from SEM backscatter images along the tensile direction, d_{TD} , tensile long transverse direction, d_{TLTD} , and short transverse direction, d_{STD} , using the directional lineal intercept method.^[26]

III. RESULTS

A. Tensile Tests

DAGG was observed during forty-four (44) of the forty-seven (47) high-temperature tensile tests performed on Mo PMB. All tests at 1823 K (1550 °C) and higher temperatures produced DAGG. Table II enumerates the tensile tests that produced DAGG at each testing temperature. Multiple tests were conducted at 1923 K and 2073 K (1650 °C and 1800 °C) to provide statistically meaningful data for analysis of the critical strain, ϵ_c , that defines the onset of DAGG. Examples of the true-stress vs true-strain data from DAGG tests at (a) 1923 K (1650 °C) and (b) 2073 K (1800 °C) are shown in Figure 2. For each temperature, tensile stress-strain data from the tests that produced DAGG at the lowest and highest critical strains are shown. The distribution of ϵ_c values at each temperature is shown by a histogram inset within the respective stress-strain plot. Each histogram displays a curve of the computed normal probability density function (PDF) spanning the 95 pct confidence interval in the ϵ_c data and a shaded region beneath it spanning the range of the standard deviation. A normal distribution function was chosen for this analysis because it provides the simplest meaningful model that reasonably represents these data. Cumulative probability distribution functions (CDFs) were calculated from the normal distributions of these ϵ_c

data. A plot of the CDFs is provided in Figure 3. Table III shows the average values of ϵ_c , ϵ_c^{avg} , and the average true stress immediately prior to ϵ_c , σ_c^{avg} , for temperatures of 2073 K and 1923 K (1800 °C and 1650 °C). At each temperature, there is a significant variation in ϵ_c between individual tests. The range of values for σ_c is small at each testing temperatures. The values of σ_c^{avg} agree with values in the literature for the steady-state flow stress of polycrystalline Mo at these temperatures.^[21,27] The values of ϵ_c for all tests that produced DAGG in Mo PMB are shown as a function of temperature in Figure 4. Data from the Mo PMA material are also shown in Figure 4 for comparison. The Mo PMA material demonstrates earlier initiation of DAGG, *i.e.*, smaller ϵ_c values, than does the Mo PMB material.

B. Morphologies of DAGG Grains

Approximately half of the halt tests were terminated quickly enough after the stress drop at ϵ_c to produce DAGG grains that did not grow through the specimen thickness. In some of these test specimens, DAGG grains were observed on only one of the two primary sheet surfaces, while others contained different DAGG grains on each of the two primary sheet surfaces. DAGG grains that did not grow through the sheet thickness are designated “surface DAGG grains,” while DAGG grains that grew through the specimen thickness are designated “through-thickness DAGG grains.” Figure 5 shows two tensile coupons containing DAGG grains that are representative of these morphologies. Both specimens were tested at 1923 K (1650 °C) and a constant true-strain rate of 10^{-4} s^{-1} . The top and bottom sheet surfaces of the tensile coupons are shown beside optical photomicrographs of specimen cross

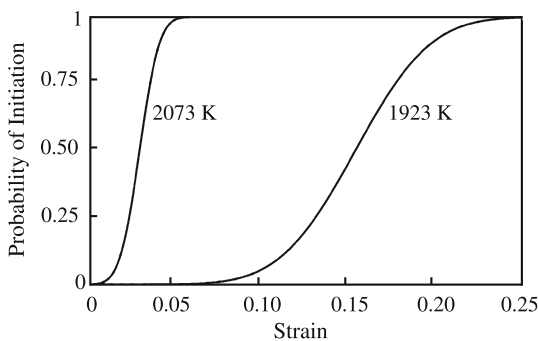


Fig. 3—Cumulative probability distribution functions (CDFs) for DAGG initiation in Mo PMB are shown as functions of strain at temperatures of 1923 K and 2073 K (1650 °C and 1800 °C).

sections: section A-A is perpendicular to the tensile long transverse direction (TLTD), and section B-B is perpendicular to the tensile direction (TD). The surface DAGG grain in Figure 5(a) is clearly visible on the top sheet surface of this specimen but does not appear on the bottom sheet surface. sections A-A and B-B of Figure 5(a) demonstrate that this DAGG grain grew readily along the specimen TD and TLTD, but not along the specimen short transverse direction (STD). The through-thickness DAGG grain in Figure 5(b) grew more readily near the sheet surfaces than near the sheet center. Section A-A reveals this in the DAGG grain’s “hourglass” shape that extends further along the TD near either sheet surface than near the sheet center.

C. Recrystallization Texture and DAGG Grain Orientations

EBSD analysis from a cross section of the Mo PMB sheet recrystallized at 1873 K (1600 °C) for two hours is shown in Figure 6. These data show the primary recrystallization texture of the Mo PMB material as pole figures and an inverse pole figure (IPF) map colored with respect to the TD. The texture at the surface of the Mo PMB material is dominated by a γ -fiber, $\langle 111 \rangle$ parallel to the STD, with a weak α -fiber, $\langle 110 \rangle$ parallel to the sheet rolling direction. Near the sheet center, the majority γ -fiber is stronger and the minority α -fiber is weaker than near the sheet surface. These are the only significant differences between the textures near the sheet surface and near the sheet center.

Figure 7 presents the EBSD data from the cross section of Figure 7 on inverse pole figures. Additionally, inverse pole figures showing the orientation of discrete

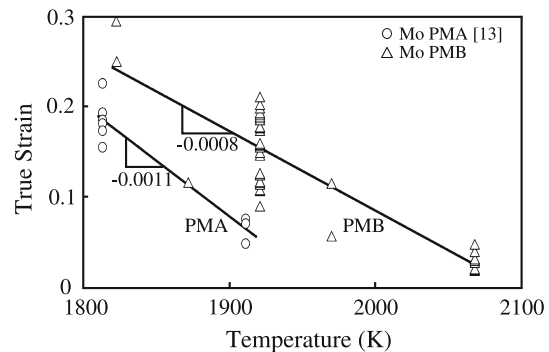


Fig. 4—The true strain accumulated in tension before DAGG initiation, ϵ_c , is shown as a function of temperature for the Mo PMA material of Worthington *et al.*^[13] and the Mo PMB material of this study.

Table III. The Values of ϵ_c^{avg} and σ_c^{avg} in Mo PMB at 1923 K and 2073 K (1650 °C and 1800 °C) Are Provided with the Standard Deviation (SDev) of Each.

T (K)	T (°C)	$\epsilon_c^{\text{avg}} \pm \text{SDev}$	$\sigma_c^{\text{avg}} \pm \text{SDev}$ (MPa)	Sample Size
1923	1650	0.15 ± 0.03 (± 22 pct)	36.0 ± 0.6 (± 1.8 pct)	29
2073	1800	0.028 ± 0.01 (± 34 pct)	22.6 ± 0.9 (± 4.0 pct)	11

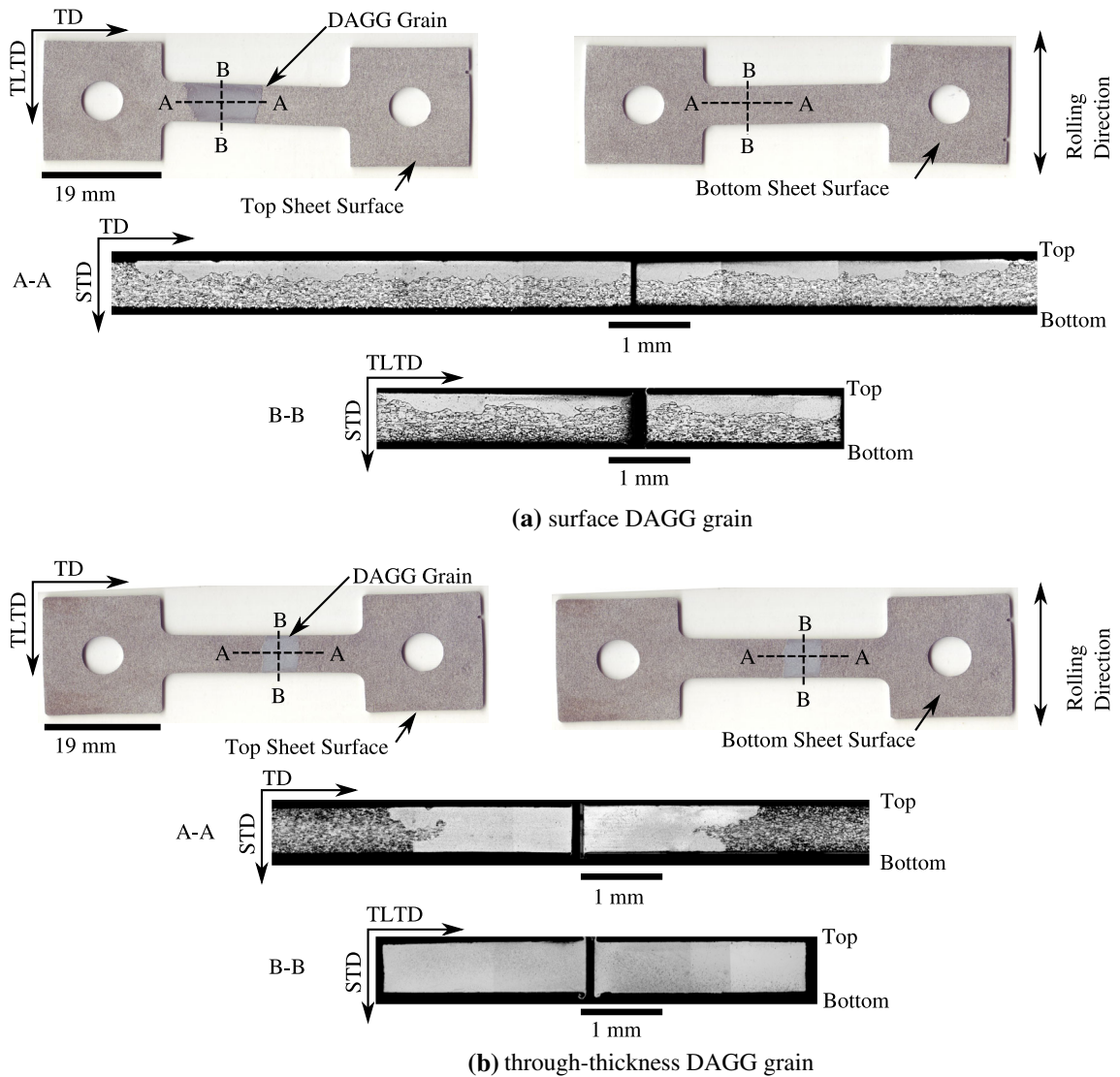


Fig. 5—Two tensile specimens with DAGG grains from the Mo PMB material are shown after testing at a constant true-strain rate of 10^{-4} s^{-1} at 1923 K (1650 °C): (a) a tensile coupon tested to a true strain of 0.12 containing a surface DAGG grain and (b) a tensile coupon tested to a true strain of 0.16 containing a through-thickness DAGG grain. The top and bottom sheet surfaces of the specimens are shown, along with cross sections A-A (TLTD normal) and B-B (TD normal). The bottom sheet surface is downward in cross sections A-A and B-B. Slight contrast variations within the DAGG grains are externally created from digital image stitching.

DAGG grains produced in Mo PMB specimens are shown. Inverse pole figures representing the recrystallization textures at the sheet surface and sheet center of recrystallized Mo PMA material and the orientations of discrete DAGG grains produced in Mo PMA^[13] specimens are shown in Figure 8. The specimen tensile axis direction (TD) of Mo PMA was parallel to the final sheet rolling direction (RD) for all tests. These figures provide easy comparison between the recrystallization textures and the orientations of DAGG grains in both the Mo PMB and Mo PMA materials.

D. Grain Sizes Through the Sheet

Directional grain sizes were measured near the sheet surface along the TD and TLTD in the undeformed grip

regions of Mo PMB specimens after testing at temperatures from 1723 K to 2073 K (1450 °C to 1800 °C). Directional grain sizes were also measured near the sheet surface along the STD in the undeformed grip region of a Mo PMB specimen after testing at 1723 K (1450 °C). Table IV provides the directional grain sizes d_{TD} , d_{TLTD} , and d_{STD} in these recrystallized, but undeformed, materials. These measurements indicate that the directional grain sizes in Mo PMB do not vary significantly between these temperatures and annealing times. For comparison, the average grain sizes in the Mo PMA material after recrystallization at temperatures from 1713 K to 1914 K (1440 °C to 1640 °C) are provided in Table V. These average grain sizes were measured using the lineal intercept method described in ASTM E112-13.

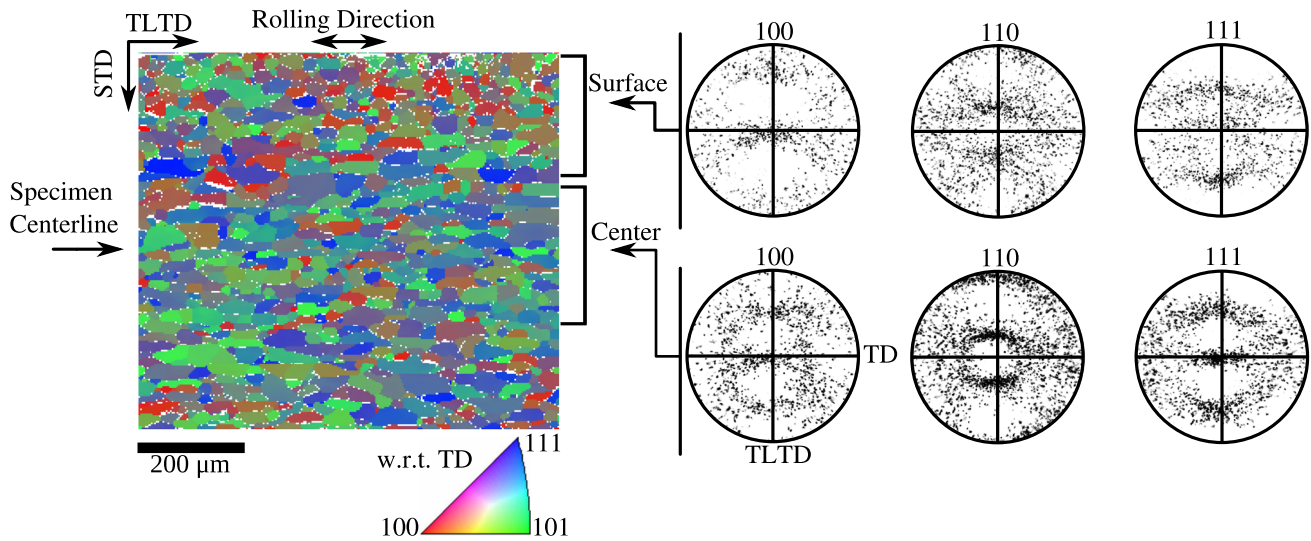


Fig. 6—EBSD data from a cross section of recrystallized Mo PMB material are shown as pole figures and as an IPF map colored with respect to the TD. Data are from a Mo PMB sheet statically recrystallized at 1873 K (1600 °C) for 2 h. Unindexed points are left as white in the IPF map.

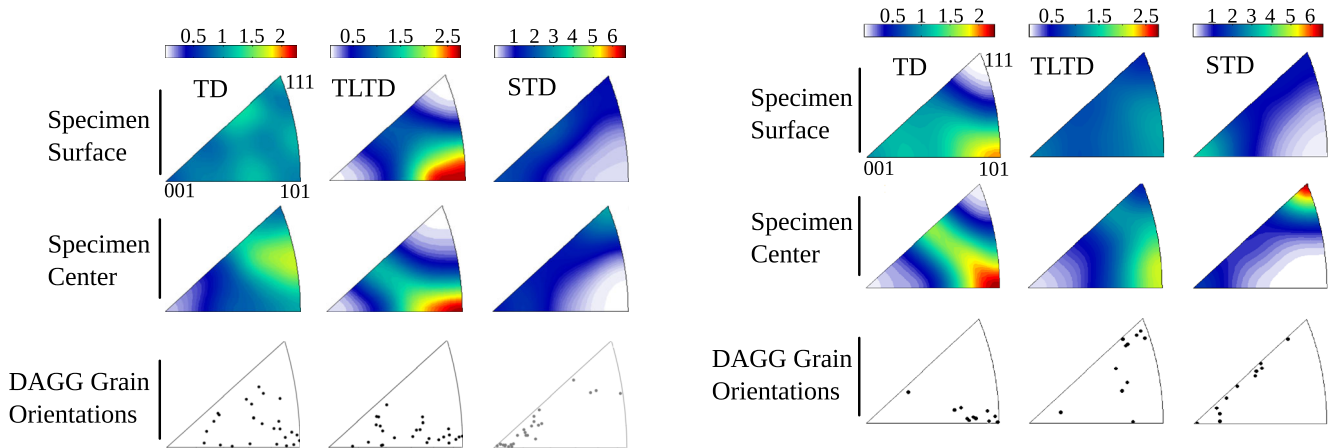


Fig. 7—EBSD data from the (top row) surface and (middle row) center of an undeformed Mo PMB sheet recrystallized at 1873 K (1600 °C) for 2 h are shown as inverse pole figures. The discrete orientations of DAGG grains observed in numerous specimens of Mo PMB after tensile tests are shown (bottom row) in inverse pole figures.

Fig. 8—EBSD data from the (top row) surface and (middle row) center of an undeformed Mo PMA sheet recrystallized at 1813 K (1540 °C) for 3 h are shown as inverse pole figures. The discrete orientations of DAGG grains observed in numerous specimens of Mo PMA after tensile tests are shown (bottom row) in inverse pole figures. These data are from reference^[13].

Sections on the TD-STD and TLTD-STD planes in the undeformed grip region of a Mo PMB tensile specimen tested at 1723 K (1450 °C) for 3 hours were characterized with backscatter electron scanning on an SEM. These are shown in Figure 9. The original sheet centerlines are indicated in these images. The centerlines are slightly offset from the bottom surfaces, labeled as the polished surface, because material was previously removed from this side for metallographic examinations. Grain sizes along the TD, TLTD, and STD were measured throughout the sheet thickness using the lineal intercept method.^[26] These measurements produced directional grain sizes d_{TD} , d_{TLTD} , and d_{STD} , respectively. Figure 10 shows (a) d_{TD} , (b) d_{TLTD} , and (c) d_{STD} as functions of the distance from the specimen centerline. Although d_{TD} and d_{STD} vary little between the sheet

center and surface, d_{TLTD} changes significantly, from approximately 35 μm near the centerline to 18 μm near the sheet surface.

IV. DISCUSSION

A. DAGG Initiation

DAGG initiated during tensile testing of all Mo PMB specimens at temperatures of 1823 K (1550 °C) and higher. The ϵ_c at DAGG initiation in Mo PMB decreases with increasing temperature, as shown graphically in Figure 4. The trend lines in Figure 4, calculated through linear regression, indicate that ϵ_c for both the Mo PMB and Mo PMA materials decreases at a similar rate with increasing temperature, approximately 10^{-3}

Table IV. Directional Grain Sizes d_{TD} , d_{TLTD} , and d_{STD} Measured Near the Sheet Surface of Mo PMB Specimens After Recrystallization Are Provided with Their Standard Deviations as Functions of Annealing Temperature, T , and Time, t

T (K)	T ($^{\circ}$ C)	t (min)	d_{TD} (μ m)	d_{TLTD} (μ m)	d_{STD} (μ m)
1723	1450	180	20 \pm 2	19 \pm 1	12 \pm 1
1723	1450	210	19 \pm 1	20 \pm 1	—
1923	1650	130	21 \pm 5	28 \pm 9	—
1923	1650	570	22 \pm 3	27 \pm 5	—
2073	1800	120	20 \pm 3	21 \pm 5	—

Table V. The Average Grain Size, \bar{d} , of Mo PMA Specimens After Recrystallization Are Provided with Their Standard Deviations as Functions of Annealing Temperature, T , and Time, t

T (K)	T ($^{\circ}$ C)	t (min)	\bar{d} (μ m)
1713	1440	180	18 \pm 1
1813	1540	180	18 \pm 1
1913	1640	180	19 \pm 1
1913	1640	480	18 \pm 1

These data are from Ref. [13].

K^{-1} . The separation between these two trendlines indicates that a higher critical strain is necessary to initiate DAGG in Mo PMB than in Mo PMA. This is somewhat surprising because these materials were produced according to the same standard. Additionally, Tables IV and V indicate that, at these temperatures, both materials have similar grain sizes. The most significant difference observed between these materials is in the sheet recrystallization texture. Variation between material production lots likely explains the difference in crystallographic texture between these materials. These orientation data, shown in Figures 7 and 8, reveal the following. Approximately twice as many grains in Mo PMA are oriented with the $\langle 110 \rangle$ axis parallel to the TD than in Mo PMB. This texture in Mo PMA corresponds with the preferred crystallographic orientation of DAGG grains, the $\langle 110 \rangle$ approximately parallel to the TD. Approximately twice as many grains in Mo PMB are oriented with the $\langle 110 \rangle$ axis parallel to the TLTD than in Mo PMA, an orientation not consistently preferred by DAGG grains. These differences in recrystallization textures between Mo PMA and Mo PMB are a likely source of the differences in ϵ_c at DAGG initiation between these materials, as will now be discussed.

The large number of tensile tests conducted at 1923 K and 2073 K (1650 $^{\circ}$ C and 1800 $^{\circ}$ C) provides sufficient sample sizes to investigate statistical variations in ϵ_c . Figure 2 demonstrates that the variation in ϵ_c at a single temperature and strain rate can be reasonably characterized by the normal distribution. This finding can be used to predict how likely DAGG initiation is for a given strain and temperature, as shown in Figure 3. The fact that DAGG initiation appears to follow a statistical distribution provides new insight into the physical mechanisms associated with DAGG. It is clear that above a minimum strain, DAGG initiation is a probabilistically determined

event. The likelihood for DAGG initiation then increases with increasing strain. Thus, a minimum strain is necessary but not sufficient for DAGG initiation. Above a minimum strain, local conditions, such as grain orientation, grain-boundary mobility, the size of grain-neighbors, and/or the difference in stored energy accumulation between neighbors will determine if DAGG initiates at any given location as strain increases. As shown in Figures 7 and 8, DAGG grains in both Mo PMA and Mo PMB are generally oriented with the $\langle 110 \rangle$ axis parallel to the TD. Figures 7 and 8 demonstrate that, within a given volume, approximately twice as many grains in Mo PMA are oriented with the $\langle 110 \rangle$ axis parallel to the TD than in Mo PMB. If grains with orientations near $\langle 110 \rangle$ parallel to the TD are the only grains selected for DAGG, DAGG initiation is approximately twice as likely at a given strain in Mo PMA than in Mo PMB. The factor of two predicted by this simple statistical argument on the availability of grains favorably oriented for DAGG agrees reasonably with the differences in ϵ_c between Mo PMA and Mo PMB shown in Figure 4, a factor also of approximately two.

B. DAGG Propagation

Figure 5 shows the morphology of DAGG grains in Mo PMB shortly after DAGG initiation. The surface grain in Figure 5(a) indicates that DAGG propagates readily along the TD and TLTD near the sheet surface. However, the failure of the DAGG grain in Figure 5(a) to penetrate through the sheet center indicates much slower propagation along the STD. The through-thickness DAGG grain in Figure 5(b) does span the sheet thickness along the STD, as well as the gage width along the TLTD. However, this DAGG grain extends further along the TD near the sheet surface than at the sheet center. This produces the hourglass shape shown in the section A-A of Figure 5(b). DAGG propagation in the Mo PMB material is, thus, significantly slower at the sheet center than near the sheet surface. Furthermore, the existence of surface grains such as that in Figure 5(a) is strong evidence that DAGG grains preferentially initiate near the sheet surface in Mo PMB.

The DAGG grain morphologies shown in Figure 5 suggest that the boundary migration rates of DAGG grains vary through the sheet thickness and possibly with direction. Current theory assumes the velocity of grain-boundary migration, v , is equal to the grain-boundary mobility, m , times the driving force for grain growth, P , ($v = m \cdot P$).^[28] Differences in v must be related to differences in the boundary mobility of

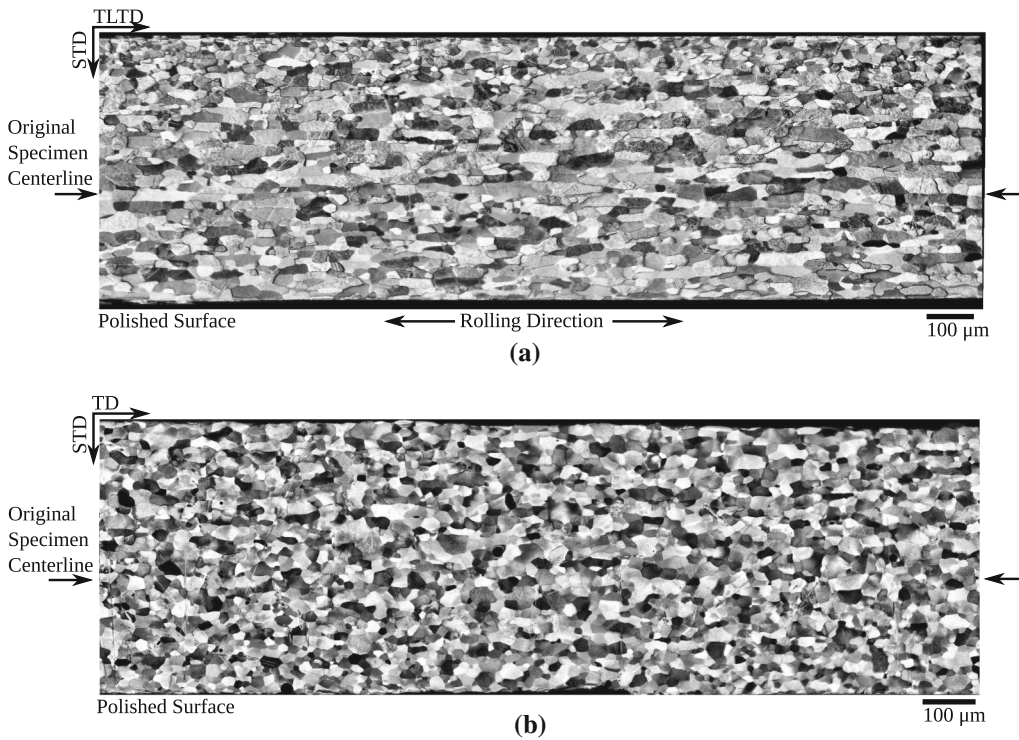


Fig. 9—Back scatter electron images of two sections from the grip region of a Mo PMB specimen recrystallized at 1723 K (1450 °C) for 3 h are shown for: (a) a section normal to the tensile direction (TD) and (b) a section normal to the tensile long transverse direction (TLTD).

DAGG and/or the driving force for DAGG between the sheet surface and sheet center. These potential causes for the observed DAGG grain morphology are now considered.

Boundary mobility arguments predict that abnormal grains are most likely to grow from minority texture components in materials with a strong texture.^[20] It is argued that this occurs because a grain from a minority component in a strongly textured material forms high-angle grain boundaries, which have high mobility, with its neighbors. This facilitates the growth of grains from minority texture components. Because DAGG occurs preferentially near the sheet surface in Mo PMB, these arguments lead to the following expectations for experimental observations:

1. A significant texture difference between the sheet surface and the sheet center.
2. DAGG grains that come from a minority texture component with respect to the sheet surface but a majority texture component with respect to the sheet center.

These form hypotheses to test against experimental data. Figure 6 demonstrates that there is a slight difference between the textures at the surface and the center of the Mo PMB sheet. It is conceivable that this slight texture difference produces the significant difference in DAGG propagation rates observed between the sheet surface and sheet center. Consider now Figure 7,

which compares DAGG grain orientations to the recrystallization textures within the sheet. The orientations of DAGG grains are more similar to the recrystallization texture near the sheet surface than that near the sheet center. These experimental observations are the opposite of those predicted above. Thus, it is unlikely that crystallographic texture has dominant control over DAGG in the Mo PMB material.

A more likely explanation for the observed DAGG grain morphologies is a variation in driving force for DAGG propagation through the sheet thickness. For the conditions under which this material was tested, grain-boundary curvature is likely to be an important driving force for grain growth.^[1,29] Grain-boundary curvature causes large grains to consume small grains and is known to promote abnormal grain growth in fine-grained microstructures.^[1,20] This driving force is proportional to the inverse of the radius of curvature between two adjacent grains. The driving force for growth from grain-boundary curvature increases as grain size decreases because smaller grains have smaller radii of curvature. If grain size varies within a microstructure, a DAGG grain will likely consume regions with the smallest grains most readily. Thus, if grain-boundary curvature is the cause of preferential DAGG near the sheet surface, then a variation of grain size through the sheet thickness, with the finest grains near the sheet surface, is expected. This hypothesis is now tested against the experimental data.

Figures 9 and 10 show that grain size varies through the Mo PMB sheet thickness. Grains near the sheet surface are, on average, significantly smaller than those near the sheet center, at least along the TLTD direction.

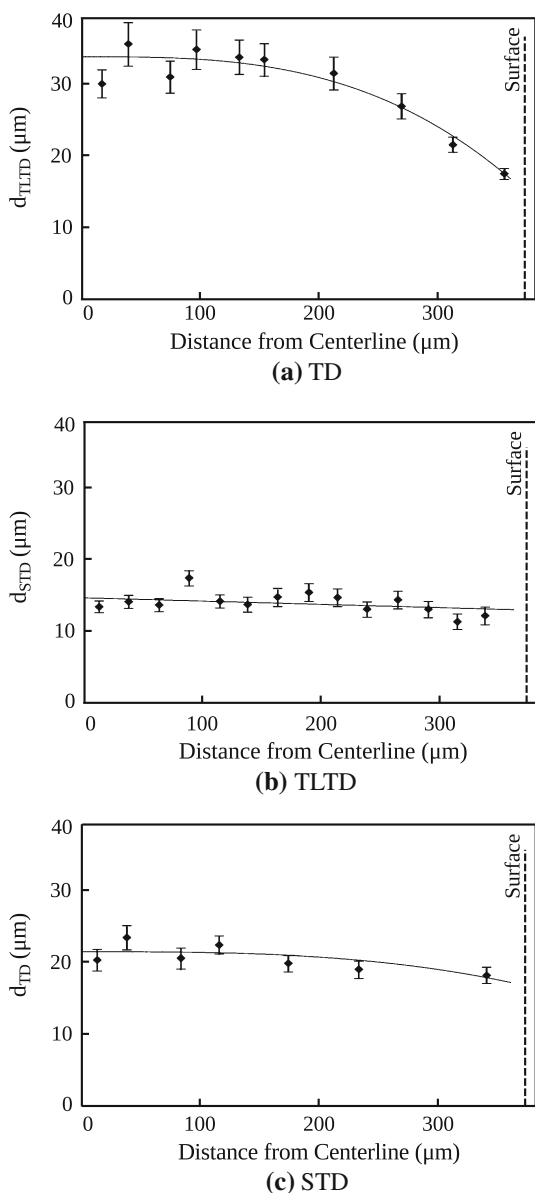


Fig. 10—The directional grain dimensions along the (a) TD, (b) TLTD, and (c) STD are shown as functions of the distance from the specimen centerline. These data were measured from a Mo PMB specimen recrystallized at 1723 K (1450 °C) for 3 h.

This supports the hypothesis for control of DAGG by grain-boundary curvature. However, more can be learned by considering the effect of grain morphology on the directionality of DAGG. The driving force, P , for a grain to consume another grain can be expressed as

$$P = \frac{\gamma}{R}, \quad [1]$$

where γ is the grain-boundary energy and R is the radius of curvature, which is related to the grain size of the smaller grain. To compare the driving forces for the consumption of surface grains to center grains, we begin by defining center grains as grains with centroids within 100 μm of the sheet centerline and surface grains as grains with centroids within 100 μm of the sheet surface. The directional sizes d_{TLTD} , d_{TD} , and d_{STD} of center and surface grains are reported in Table VI. Assuming constant grain-boundary energy throughout the microstructure,

$$\frac{P^s}{P^c} = \frac{R^c}{R^s}, \quad [2]$$

where P^c and P^s are the driving forces for boundary migration at the sheet center and surface, respectively, and R^c and R^s are the radii of curvature for grain boundaries at the sheet center and surface, respectively. The ratio P^s/P^c thus shows how the driving force for DAGG from grain-boundary curvature varies through the sheet thickness. Because the grains are approximately ellipsoidal in shape, the driving forces from grain-boundary curvature for growth are necessarily directional. Assuming ellipsoidal grains, the directional grain sizes reported in Table VI provide the axes of the ellipsoids and enable the calculation of local curvature. The maximum and minimum curvatures, κ_1 and κ_2 , for a specific direction can be used to calculate an average R for use in Eqs. [1] and [2] as

$$R = \left[\frac{1}{2}(\kappa_1 + \kappa_2) \right]^{-1}. \quad [3]$$

The results of these calculations are provided in Table VI.

Table VI establishes several key points concerning the driving force for grain growth from grain-boundary curvature in Mo PMB. Because the grain dimension d_{TLTD} is significantly smaller for surface grains than for center grains, the driving forces from grain-boundary curvature for DAGG along the TD and STD are significantly larger near the sheet surface than near the

Table VI. The Grain Sizes and Calculated Average Directional Radii of Curvature Along the TLTD, TD, and STD Are Reported for the Undeformed Grip Region of a Mo PMB Tensile Specimen Tested at 1723 K (1450 °C) for 3 h

Direction	d^s (μm)	d^c (μm)	R^s (μm)	R^c (μm)	P^s/P^c
TLTD	20.0 ± 0.7	32.6 ± 1.2	2.7 ± 0.8	2.4 ± 0.5	0.9 ± 0.1
TD	18.8 ± 1.1	22.0 ± 0.9	3.0 ± 0.9	4.4 ± 0.9	1.5 ± 0.1
STD	12.4 ± 0.5	15.4 ± 0.4	7.6 ± 2.3	10.8 ± 2.5	1.4 ± 0.1

The ratio P^s/P^c is also given. Superscripts s and c in this table refer to center and surface grains, respectively.

sheet center. Conversely, the driving force for growth along the TLTD does not vary much through the sheet thickness. Finally, the average radii of curvature for both center and surface grains in the TD and TLTD are much smaller than in the STD. These geometric calculations predict the following:

1. DAGG throughout the material will progress most rapidly along the TLTD,
2. DAGG will progress more rapidly along the TD and STD near the sheet surface than near the sheet center, and
3. DAGG will progress more slowly along the STD than along either the TD or TLTD.

These predictions are exactly reflected by the morphology of DAGG grains observed in Mo PMB. Shortly after initiation, DAGG grains completely span the TLTD, as is shown in the view B-B for both DAGG grains in Figure 5. Figure 5(b) establishes that DAGG progresses more rapidly along the TD near the sheet surface than near the sheet center. Finally, the surface grain in Figure 5(a) indicates that DAGG progresses much more slowly along the STD than along the TD or TLTD. These findings demonstrate that the primary driving force for DAGG in the Mo PMB material is grain-boundary curvature.

V. CONCLUSIONS

DAGG is an abnormal grain growth phenomenon that occurs during plastic deformation at elevated temperatures. DAGG was used to produce large single crystals in a commercial-purity Mo material, Mo PMB, at temperatures between 1823 K and 2073 K (1550 °C and 1800 °C). The critical strain at DAGG initiation and the morphology of DAGG grains in this material were investigated. It is concluded that

1. The critical strain for DAGG initiation decreases approximately linearly with increasing temperature.
2. The critical strain for DAGG initiation varies significantly for a given testing temperature and strain rate. This variation follows a normal distribution.
3. Texture affects the critical strain for DAGG initiation. An increase in the fraction of grains oriented with the $\langle 110 \rangle$ along the tensile axis decreases the critical strain for DAGG initiation.
4. Variations in local crystallographic texture do not appear to influence DAGG propagation.
5. The propagation of DAGG is observed to be driven primarily by grain-boundary curvature with DAGG grains preferentially growing into the finest-grained polycrystalline regions.

ACKNOWLEDGMENTS

The authors gratefully acknowledge support from the National Science Foundation for this work under Grant DMR-1105468 and for equipment acquired under DMR-9974476.

REFERENCES

1. J.G. Byrne: *Recovery, Recrystallization, and Grain Growth*, The Macmillan Company, New York, 1965, p. 106.
2. M. Hillert: *Acta Metall.*, 1965, vol. 13, pp. 227–38.
3. F. Humphreys and M. Hatherly: *Recrystallization and Related Annealing Phenomena*, 2nd ed., Elsevier, New York, 2004, pp. 24–25.
4. V. Randle: *Philos. Mag. A*, 1993, vol. 67, pp. 1301–13.
5. C. Briant, F. Zaverl, and W. Carter: *Acta Metall. Mater.*, 1994, vol. 42, pp. 2811–21.
6. S. Lee, D. Yoon, and M. Henry: *Acta Mater.*, 2000, vol. 48, pp. 3071–80.
7. T. Fujii, Y. Hiraoka, and R. Watanabe, United States Patent No. 4,491,560, January 1 1985.
8. K. Takebe and Y. Hiraoka: Japan Patent No. JP6248384, September 6, 1990.
9. D. Dorner, S. Zaefferer, L. Lahn, and D. Raabe: *J. Magn. Magn. Mater.*, 2006, vol. 304, pp. 183–86.
10. C. Musiol: *Met. Technol. (Lond.)*, 1976, vol. 3, pp. 173–82.
11. A.D. Rollett, A.P. Brahme, and C. Roberts: *Mater. Sci. Forum*, 2007, vol. 558, pp. 33–42.
12. J. Ciulik and E. Taleff: *Scripta Mater.*, 2009, vol. 61, pp. 895–98.
13. D.L. Worthington, N.A. Pedrazas, P.J. Noell, and E.M. Taleff: *Metall. Mater. Trans. A*, 2013, vol. 44A, pp. 5025–38.
14. N.A. Pedrazas, T.E. Buchheit, E.A. Holm, and E.M. Taleff: *Mater. Sci. Eng. A*, 2014, vol. 610, pp. 76–84.
15. A. Rollett and W. Mullins: *Scripta Mater.*, 1997, vol. 36, pp. 975–80.
16. Y.C. Zhu, J.H. Mao, F.T. Tan, and X.L. Qiao: *Appl. Mech. Mater.*, 2012, vol. 127, pp. 89–94.
17. T.A. Bennett, P.N. Kalu, and A.D. Rollett: *Microsc. Microanal.*, 2011, vol. 17, p. 362.
18. A. Agnoli, M. Bernacki, R.E. Logé, J.-M. Franchet, J. Laigo, and N. Bozzolo: *Superalloys 2012: The 12th International Symposium on Superalloys*, 2012, pp. 73–82.
19. P. Lin, G. Palumbo, J. Harase, and K. Aust: *Acta Mater.*, 1996, vol. 44, pp. 4677–83.
20. F. Humphreys: *Acta Mater.*, 1997, vol. 45, pp. 4231–40.
21. J. Ciulik and E. Taleff: *Mater. Sci. Eng. A*, 2007, vol. 463, pp. 197–202.
22. ASTM International: *Standard Specification for Molybdenum and Molybdenum Alloy Plate, Sheet, Strip and Foil, Standard Designation B 306–03*, ASTM International, West Conshohocken, 2003.
23. ASTM International: *Standard Test Method for Determination of Carbon in Refractory and Reactive Metals and Their Alloys, Standard Designation E 1941–04*, ASTM International, West Conshohocken, 2008.
24. R. Barto and L. Ebert: *Metall. Trans.*, 1971, vol. 2, pp. 1643–49.
25. HKL Channel 5, Oxford Instruments PLC, Oxon.
26. ASTM International: *Standard Test Methods for Determining Average Grain Size, Standard Designation E 112–13*, ASTM International, West Conshohocken, 2013.
27. W. Green, M. Smith, and D. Olson: *Trans. Metall. Soc. AIME*, 1959, vol. 215, pp. 1061–66.
28. G. Gottstein and L. Shvindlerman: *Acta Metall. Mater.*, 1993, vol. 41, pp. 3267–75.
29. G. Gottstein and L.S. Shvindlerman: *Grain Boundary Migration in Metals: Thermodynamics, Kinetics, Applications*, 2nd ed., CRC Press, New York, 2009, pp. 140–144.